15-cm Mercury Multipole Thruster

Glen R. Longhurst* and Paul J. Wilbur†
Colorado State University, Fort Collins, Colo

A 15-cm multipole ion thruster was adapted for use with mercury propellant. During the optimization process, the magnetic field was found to: 1) define the region where the bulk of ionization takes place; 2) influence the magnitudes and gradients in plasma properties in this region; and 3) control impedance between the cathode and main discharge plasmas in hollow cathode thrusters. The mechanisms for these functions are discussed. Data from SERT II and cusped magnetic field thrusters are compared with those measured in the multipole thruster. The performance of this thruster is shown to be similar to that of the other two thrusters. Means of achieving further improvement in the performance of the multipole thruster are suggested.

Introduction

IT has been observed by many investigators[1-5] that the magnetic field configuration within an ion thruster discharge chamber plays a prominent role in determining thruster performance. It has been found[1] that in addition to containing primary electrons long enough to provide significant ionization probability, a magnetic field which diverges toward the screen electrode provides more uniform ion density there. It was suggested by King, et al.,[5] and substantiated by Beattie[3] that a critical field line passing from the downstream end of the cathode pole piece to the anode pole piece, when revolved about the thruster axis to form a surface of revolution, represents the upstream boundary of the region within which the bulk of the propellant ionizations occur. The screen grid forms the downstream boundary of this region which is commonly called the primary electron region. The distance between the surface of revolution of the critical field line and the screen grid at a given radius determines the relative ionization probability for a neutral propellant atom at that radius. Beattie[2] also found that there was a strong interrelationship between the proximity of the anode to that critical field line and the plasma properties obtained in the discharge chamber, particularly Maxwellian electron temperature.

Isaacson and Kaufman[6] reported a multipole magnetic field thruster design which yielded a primary electron region that was essentially cylindrical in shape. It was shown to operate efficiently using argon and xenon as propellants and to have a very flat beam current density profile. Because it appeared to operate as efficiently as could be expected with these propellants, and because this design can be scaled easily to various sizes, an investigation of its use with mercury propellant was undertaken. This multipole design had not been operated on mercury nor had it been operated using a hollow cathode, so some optimization of the chamber was required before meaningful comparisons could be made against other thruster designs. Parameters varied during this optimization process included the discharge chamber length, the field strength, and the axial location of electron injection from the cathode discharge chamber into the main discharge chamber.

Presented as Paper 78-682 at the AIAA/DGLR 13th International Electric Propulsion Conference, San Diego, Calif., April 25-27, 1978; submitted May 18, 1978; revision received Sept. 19, 1978. This paper is declared a work of the U.S. Government and therefore is in the public domain.

Index categories: Electric and Advanced Space Propulsion; Engine Performance.

*Graduate Research Assistant. Student Member AIAA.

†Associate Professor, Department of Mechanical Engineering. Member AIAA.

Apparatus and Procedure

Figure 1 is a schematic drawing of the 15-cm diameter axisymmetric multipole thruster configuration used during most of this study. Proper operation of the device depends on the establishment of magnetic fields between pole piece pairs straddling each of the anodes shown in Fig. 1. These anodes serve to remove low-energy electrons from the discharge chamber as high-energy (primary) electrons are resupplied from the cathode. The construction details of the side wall and upstream sections, as well as the magnetic field characteristics obtained, were the same as those for the thruster used by Isaacson and Kaufman[6] during their tests with argon and xenon. The side wall sections are 2.7 cm from pole to pole and are designed so they can be added or removed to vary the discharge chamber length.

The thruster was fitted with a conventional mercury feed system and a hollow cathode. The cathode was a 3-mm-diam. tantalum tube with a thoriated tungsten orifice plate having a 0.38-mm diam orifice. A tantalum foil insert coated with chemical R500‡ (barium carbonate-strontium carbonate) was located inside the cathode, immediately upstream from the cathode orifice plate. A resistance heater was fixed to the cathode tube adjacent to the tip. The mercury propellant flow rate was controlled to the main propellant plenum and the hollow cathode separately by conventional, sintered tungsten, mercury vaporizers. Compensated high perveance dished grids, having a screen grid open area fraction of 0.67 and an accelerator open area fraction of 0.54, were used. A cold grid spacing of 0.79 mm was maintained with mica spacers. The screen potential was 1000 V while accelerator grid potential was -500 V on all tests. The magnetic baffle assembly shown in Fig. 1 was used to control the baffle aperture impedance and, hence, the primary electron flow into the main discharge region for most of the tests conducted. The need for this magnetic baffle developed, however, as a result of preliminary tests which will be discussed in a succeeding section of this paper. The cathode chamber (consisting of the magnetic baffle assembly, cathode, keeper, and heater) could be moved axially during thruster operation. By positioning this chamber at different axial positions the axial location of primary electron injection into the main discharge region could be varied.

With the magnetic baffle installed, the thruster length was varied and thruster performance measurements were made. Thruster length was varied for these tests by operating with 1, 2, 3, and 4 side wall sections. The cathode chamber was extended from a position flush with the upstream pole piece to one approaching either the grids or a point 5 cm into the discharge region, whichever was less, for each of these test configurations. Total propellant flow was maintained within

‡J.T. Baker Chemical Co., Phillipsburg, N.J.

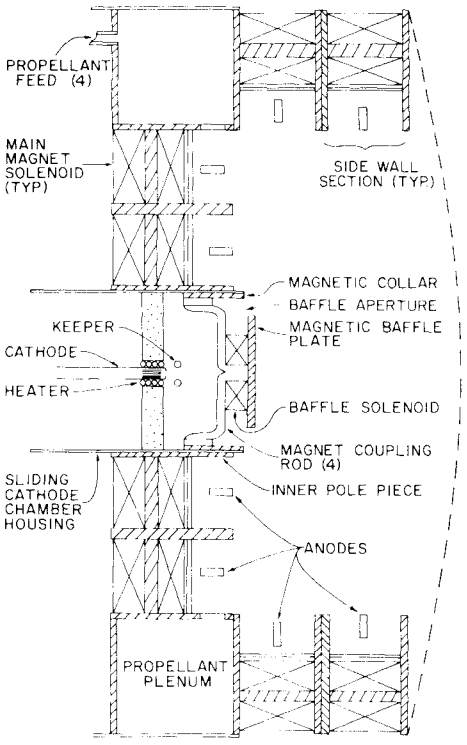

Fig. 1 15-cm multipole mercury ion thruster.

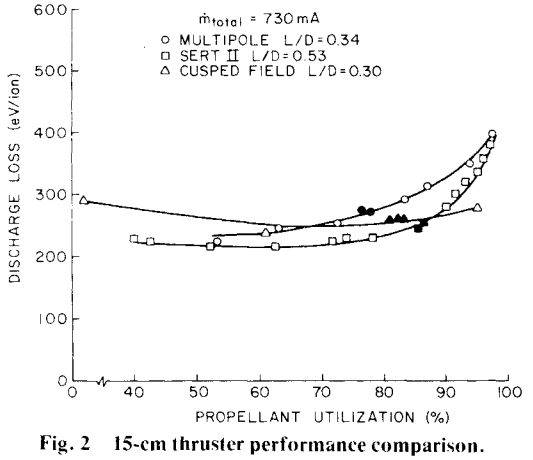

Fig. 2 15-cm thruster performance comparison.

1% of 730 mA eq. while data were being taken. The cathode propellant flow rate was adjusted over the range of 3.8-8.5% of the total flow to maintain the discharge voltage near 37 V and to facilitate stable operation. Tests were conducted in a 1.2-m diam by 4.6-m long vacuum facility and pressures were in the high 10^{-6} Torr range during data collection.

Plasma properties were measured using a Langmuir probe which could be moved throughout the main discharge chamber. Analysis of the probe chraracteristics was accomplished using the computer program developed by Beattie.[7] Doubly charged ion current density measurements were made in the beam using an articulated $E \times B$ momentum analyzer[8] located 68 cm downstream from the grids. A Faraday probe which could be swept through the beam on an axial plane 0.5 cm downstream from the grids was used to obtain ion beam current density profiles.

Results and Discussion

Performance

It was found that the 15-cm mercury multipole thruster gave performance similar to SERT II and cusped magnetic field thrusters once it had been optimized with respect to the

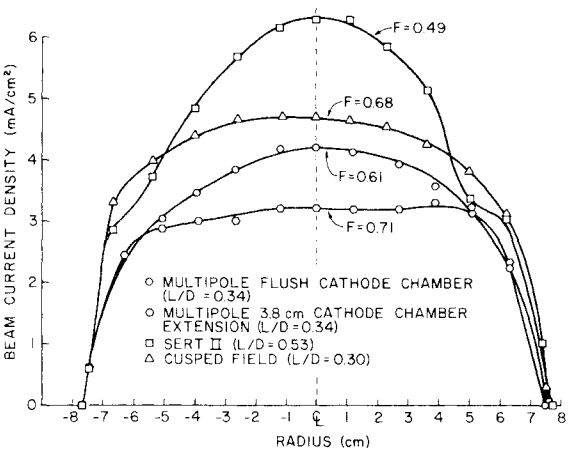

Fig. 3 Ion beam profile comparison.

number of side wall sections, the magnetic field intensity, and the axial location at which primary electrons were injected into the main discharge chamber. A comparison of the performance of these three optimized thruster configurations, each operating at the same propellant flow rate (730 mA eq.), is shown in Fig. 2. The solid symbols on this figure correspond to operation at a 37 V discharge potential. The quantity L/D used in the legend is the length-to-diameter ratio of each thruster. Length, as used here, is the distance between the screen grid plane and the plane of the downstream edges of the upstream pole pieces. For the SERT II thruster, the upstream pole piece is the cathode pole piece.

While the performance is comparable for these three discharge chamber configurations, that of the multipole thruster is seen in Fig. 2 to be slightly poorer. It is expected that further improvements in multipole thruster performance can be achieved through additional optimization, but the extent of these improvements would be sufficiently small that the other thrusters will continue to show better performance. The reason for this is associated with the shape of the region in which the bulk of the ions are produced. In the SERT II thruster this production tends to concentrate along the thruster centerline and in the region close to the screen grid. The screen grid tends to present a relatively large solid angle to ions produced in these regions so the probability of escape for the ions is also relatively large. In the multipole design, on the other hand, ion production in the upstream corner of the discharge chamber and along the side walls becomes significant. The screen grid tends to present a smaller solid angle to these ions so their chances of escape through the screen grid are reduced. This in turn should result in the higher discharge losses observed for the multipole design.

Figure 3 presents a comparison of ion beam current density profiles obtained with the multipole thruster with those measured in the cusped magnetic field and SERT II thrusters operating at conditions defined by the solid symbols of Fig. 2. The flatness parameter corresponding to each curve, defined as the ratio of average-to-peak beam ion current density, is identified by the symbol F. The most peaked profile is observed for the SERT II thruster ($F=0.49$), and the flattest is observed for the multipole thruster in which the cathode chamber was extended 3.8 cm downstream toward the screen grid ($F=0.71$). The lower current densities shown for the multipole thruster reflect the lower beam current and, hence, lower propellant utilization obtained with this design.

Operating conditions and performance data obtained with optimized multipole, cusped magnetic field and SERT II thrusters at the solid symbol data points of Fig. 2 are listed in Table 1. These data show the doubly charged ion current ratio and the flatness parameter for the doubly charged ions, both measured in the ion beam of the multipole thruster, are intermediate between values observed for the SERT II and the

Table 1 Comparison of mercury thruster performance

	Multipole	SERT II	Cusped field
Hardware			
Thruster length-to-diameter ratio	0.34	0.53	0.30
Operating conditions			
Screen (accel) potential, kV	1.0(−0.5)	1.0(−0.5)	1.0(−0.5)
Propellant flow, mA	730	725	730
Discharge current, A	4.0	4.06	4.3
Discharge voltage, V	36.6	37.5	36.7
Performance data			
Beam current, mA	548	654	625
Discharge loss, eV/ion	283	239	256
Propellant utilization	0.73	0.87	0.84
Beam flatness	0.61	0.49	0.68
Doubly-to-singly charged ion current ratio	0.064	0.081	0.052
Doubly charged ion beam flatness	0.34	0.27	0.38

cusped field thruster. It was observed with the multipole thruster that extending the cathode chamber downstream to the 3.8 cm location reduced the doubly charged ion content of the ion beam substantially. This suggests that structure, such as a cathode chamber, extended close to the grids, while it degrades performance, also reduces the centerline doubly charged ion density substantially. This apparently occurs because the cathode potential surface serves to collect and neutralize both doubly and singly charged ions, thereby reducing their local density.

During the process of optimizing the performance of this thruster, several intersting phenomena and thruster characteristics were observed. While they may not impact directly on the performance of this thruster compared to other designs, they provide some physical understanding of thruster phenomena, and they will, therefore, be discussed in the following sections.

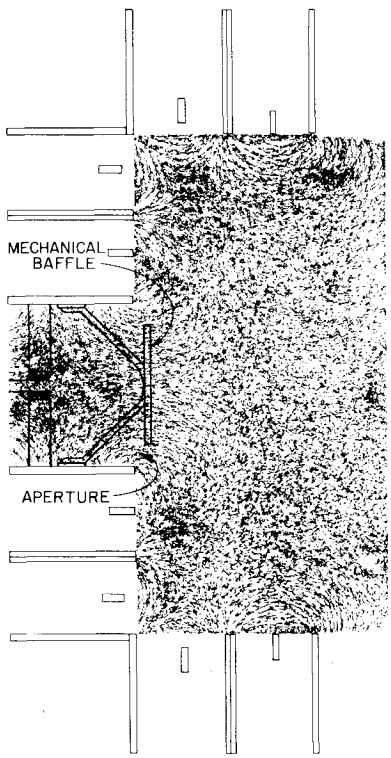

Fig. 4 Iron filings map, upstream nonmagnetic baffle assembly.

Magnetic Effects at the Cathode

Initially, the cathode chamber was fitted with a simple mechanical, nonmagnetic baffle similar to the one used on SERT II. This baffle was intended to separate the cathode chamber plasma from the main discharge plasma by inducing a potential difference through the baffle aperture. With this baffle installed, however, and with the baffle aperture positioned at the upstream end of the discharge chamber, as shown in Fig. 4, it was observed that a disproportionately large fraction of the ionization was taking place in a very small region near the innermost anode at the upstream end of

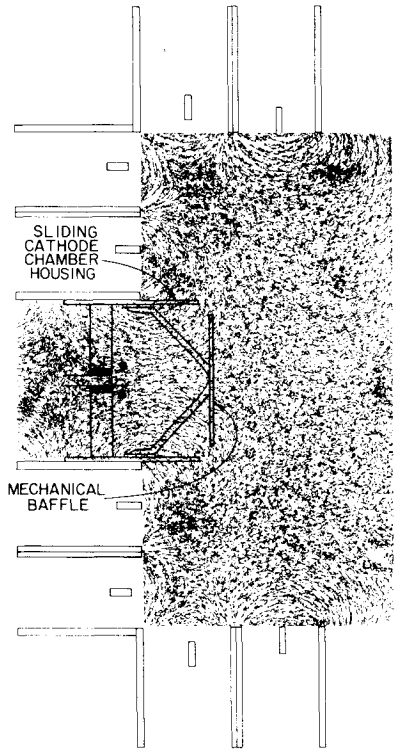

Fig. 5 Iron filings map, downstream nonmagnetic baffle assembly.

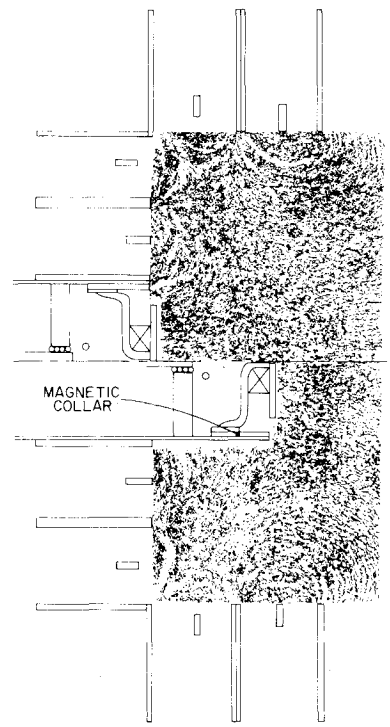

Fig. 6 Iron filings map-composite magnetic baffle assembly.

the discharge chamber. Because the ionization was not distributed more uniformly over the discharge chamber, performance was poor. The cathode chamber housing was subsequently extended downstream to the position indicated in Fig. 5, so primary electrons would be injected into a region where they would not be immediately captured by the magnetic fringe field from the inner pole piece and drawn to the innermost anode. In this configuration it was discovered that the impedance in the baffle aperture could not be adjusted to effect proper primary electron production and injection into the main discharge chamber. With a range of cathode flow rates and aperture areas between the mechanical baffle and the sliding chamber housing (Fig. 5), it was found that the potential drop developed across the baffle aperture was insufficient. As a result, the potential drop would be induced either at the cathode itself or across the magnetic fields protecting the anodes. In either case, poor performance was the result.

The phenomena which brought about this poor performance may be explained by considering the changes in magnetic fringe fields in the baffle aperture region associated with cathode chamber motion. Figure 4 shows the iron filings map of the magnetic field in a thruster having two side wall sections and the nonmagnetic baffle assembly. This figure shows that electrons leaving the cathode chamber through the baffle aperture must cross magnetic field lines. Because the magnetic field lines are essentially perpendicular to the direction of electron flow, the magnetic field provides an impedance across which the potential difference responsible for accelerating the elctrons to primary electron energies is sustained. Figure 5 shows that same magnetic field with the cathode chamber moved 2 cm downstream. With the cathode assembly in this location, not only is the magnetic field in the vicinity of the aperture weaker in intensity, but the field lines lie largely in the same direction as the electron current. Impendance due to the magnetic field is thus virtually eliminated, and control of the baffle impedance at the proper value becomes essentially impossible.

Figure 6 shows the magnetic field configuration realized when the discharge chamber is equipped with a magnetic baffle. The upper half of this figure shows the magnetic field configuration when the cathode aperture is flush with the innermost pole piece; the lower half is the iron filings map obtained with a cathode chamber extension of 3.8 cm. The major effect of the magnetic baffle on the magnetic field within the main discharge chamber occurs at the baffle aperture. Although it is not immediately apparent from Fig. 6, the magnetic field in the aperture region tends, in this case, to be perpendicular to the direction of electron flow for both cathode region positions. With the cathode chamber extended as in the lower half of Fig. 6, the field shape elsewhere in the main discharge chamber differs slightly from that observed in Fig. 5. The field near the innermost pole piece in Fig. 6 appears to be somewhat more widely dispersed, and field lines tend to go directly into the side of the cathode chamber where the magnetic collar is located.

When the magnetic baffle was positioned flush with the innermost pole piece, little or no baffle magnet current was required to effect efficient thruster operation. As the cathode chamber was extended farther and farther into the discharge chamber, away from the innermost pole piece, the baffle magnet current required to maintain the desired discharge voltage and an efficient thruster operating condition increased. These experiments demonstrated that a magnetic field is required across the baffle aperture to effect the voltage drop across which primary electron acceleration is achieved, supporting similar observations by Knauer et al.,[1] and Wells.[9] When electron injection is to be accomplished at a point in the discharge chamber where magnetic field lines do not cross the electron flow path, a magnetic baffle is required to achieve proper operation.

Cathode Position Effects

Once the proper aperture impedance was established, it was found that the point of electron injection into the main discharge chamber did not influence discharge loss and utilization levels substantially, unless the injection occurred on magnetic field lines which prevented uniform distribution of the electrons throughout the chamber. Putting the cathode assembly far downstream, however, did degrade performance slightly because the cathode assembly: 1) displaced some volume in which ionizing reactions could have otherwise taken place and 2) provided additional surface on which recombination could occur. Plasma property data taken with the cathode assembly extended confirmed the local depletion of ion densities near the centerline caused by the presence of the cathode chamber. Figure 7 shows how the ion beam profile is altered as the cathode chamber is moved downstream into the discharge chamber of a thruster that is two side sections long. Although the 3.8 cm cathode extension results in the flattest ion beam profile of the several configurations tested, it is not preferred because it results in a 3% loss in propellant utilization over that obtained with the flush configuration.

Discharge Current Distribution

The distribution of the discharge current between the anodes in the multipole thruster is controlled by the depth and intensity of magnetic fields shielding the anodes and by electron density distributions within the discharge chamber.[6] Figure 8 shows how current drawn to each of the four anodes of the optimized design varies with the position of the cathode chamber. The ordinate of Fig. 8 represents measured current drawn by a given anode divided by the radius from thruster centerline of that anode. All anodes have the same face width presented to the plasma, so dividing anode current by the radius of the anode in question yields a number representative of the discharge current density at that anode. Anode

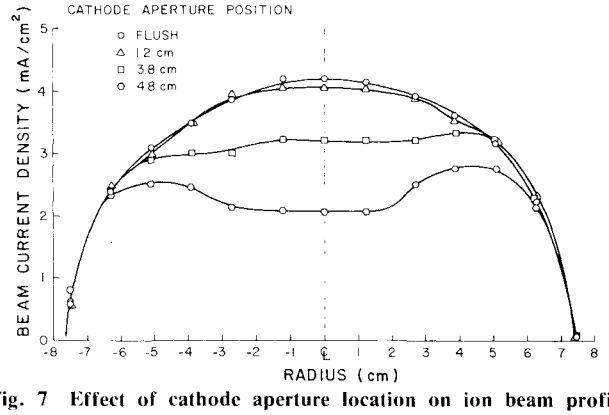

Fig. 7 Effect of cathode aperture location on ion beam profile (multipole thruster).

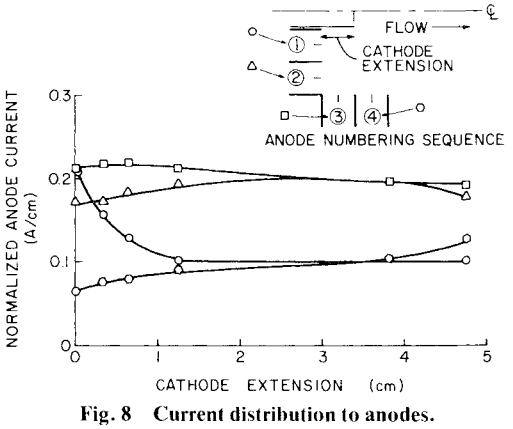

Fig. 8 Current distribution to anodes.

numbering begins with the anode closest to the cathode chamber and proceeds around the chamber periphery (Fig. 8 inset).

The number one anode is most strongly influenced by cathode extension. When the cathode aperture is flush with the upstream pole pieces, some of the electrons are injected within the fringe field which protects this anode (see Fig. 6). Their path to the number one anode is thus more direct (they need traverse less magnetic flux to reach it) than when electrons are injected into the center of the chamber. Anodes 2, 3, and 4 are nearly unaffected by cathode location. The slight rise in the current to these anodes with cathode extension is required to compensate for the corresponding drop in current to anode 1 as the cathode chamber is moved forward and the sum of current to all anodes is held constant. The downstream anode was found to have much lower currents than other side wall anodes for all thruster configurations tested. This occurs because the conductivity of the plasma across a magnetic field protecting an anode is inversely proportional to the line integral of the perpendicular component of the magnetic field intensity from the central plasma to the anode,[6] and this quantity is greater for the downstream anode. This reduced conductivity results from the greater depth of magnetic field penetration into the main discharge region for the downstream section (a condition which can be seen readily in Figs. 4-6 for the four-anode configuration). Hence, even though the total magnetic flux between the pole pieces of the downstream section is nearly the same as that between other sections, the integral is greater because more flux lines lie interior to that anode and they are more dispersed. Consequently, less current is conducted. It should be noted that the decline in the current to anode 1 is also partially due to the same effect. As previously noted and shown in Fig. 6, the fringe field in the vicinity of anode 1 becomes somewhat more widely dispersed as the cathode chamber is extended. The impedance between this anode and the plasma is thereby increased, and anode current goes down. This decline in current to anode 1 with cathode chamber extension was observed on all thruster configurations tested.

It is believed that further improvements in performance could be realized if magnetic fields and/or anode positions were adjusted so equal current densitites were drawn to each anode. The first attempt at this optimization – the recessing of anodes 2 and 3 to reduce the current drawn to them – was carried out by Isaacson[6] on the xenon and argon versions of this thruster. The 2.5-mm anode recess behind the pole piece edge that he recommended was incorporated in this thruster, but it appears some additional recessing is required to equalize the current density to each anode.

Beam Flatness

The flatness of the outer part of the beam current density profile is also influenced by the just-mentioned protrusion of the magnetic fringe field of the downstream side wall section into the discharge chamber. Beattie[3] showed that essentially the same effect in the cusped field thruster was responsible for diminution of the beam current density toward the outer radius of the beam. Qualitatively, this occurs because the high-energy electrons are restrained from that region near the downstream end near the thruster walls. As a result, more ionization takes place toward the center than near the walls of the discharge chamber at the downstream end, and plasma density at the screen is higher toward the center. This results in the beam profiles of Fig. 7 rather than the very flat ones anticipated with a cylindrical primary electron region as observed by Knauer et al.[1] in a radial field thruster, and by Isaacson and Kaufman[6] and Robinson and Kaufman[10] in multipole thrusters. The latter two studies used thrusters with more side sections, where the magnetic field protrusion effect was less observable in ion filings maps and the resulting beam diminution less apparent.

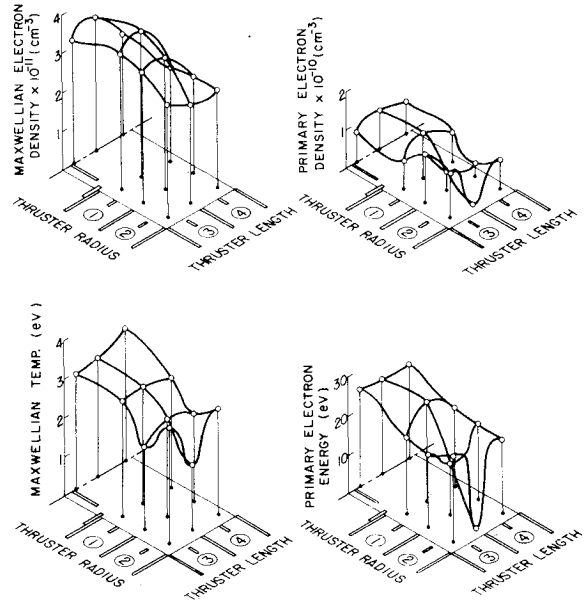

Fig. 9 Mercury multipole plasma properties.

Plasma Properties

The results of Langmuir probe measurements in the two side wall section multipole configuration with the cathode chamber extended 3 mm are shown in Fig. 9. Toward the center of the discharge chamber the plasma properties are observed to be well behaved and fairly uniform. Toward the side walls, however, there are strong perturbations due probably to the influence of the magnetic fields and anodes there. Note that near the pole piece between anodes 3 and 4 primary electrons appear to vanish, whereas near the adjacent anodes the values for primary electron density and energy are higher. A similar though less pronounced effect on primary energy appears near the pole piece between anodes 1 and 2. Maxwellian temperature is also depressed at those same locations. Compared to the SERT II and cusped field thrusters, the mean Maxwellian electron density is high and the mean temperature is low in the multipole thruster. Beattie's study[3] of the effect of anode-critical field line separation distance on plasma properties and thruster performance suggests that the local protective magnetic fields should be increased or anodes 2 and 3 should be recessed more to increase electron temperature and improve performance. Unfortunately, increases in magnetic field intensity were precluded during these tests by the onset of instabilities.

Drawing detailed conclusions from the strong variations in energy-related plasma properties (temperature and primary energy) near the pole pieces would require Langmuir probe measurements with very accurately positioned probes. Attempts to do this were not completely successful, although probe measurements at 4-mm intervals did show that dramatic variations in plasma properties occur near the pole pieces. In the central, essentially field-free region of the thruster, on the other hand, these plasma properties were uniform. Qualitatively this suggests that sharp gradients in plasma properties occur where magnetic field intensities are high. This qualitative correlation is supported by data from cusped and divergent field thrusters in which energy-related plasma properties appear to to vary gradually throughout the relatively low magnetic field intensity central core of the discharge chamber. All of these observations tend to support the theory that energy-related plasma properties tend to be constant along magnetic field lines-of-force, a concept that is argued quantitively in Ref. 11.

Visual observations of the thruster during operation revealed regions of relatively intense luminosity near the pole pieces between anodes 1 and 2 and anodes 3 and 4. The reason for this is not apparent.

Conclusions

As a result of optimization studies on the 15-cm multipole mercury thruster, three distinct functions may be associated with the magnetic fields within an ion thruster discharge chamber:

1) The magnetic field lines which serve as guiding centers for primary electrons determine where the bulk of ionization takes place. When the fields are so distributed that primary electrons do not have access to certain regions of the thruster discharge chamber, a corresponding reduction in local ionization rate results, which is manifested in plasma property variations and beam current density profiles.

2) There appears to be a strong interrelationship between plasma properties and magnetic fields. Plasma property maps reflect variations which are spatially correlated with magnetic field variations. A relationship between bulk average plasma properties and the geometric arrangement of critical field lines relative to anode surfaces is also observed.

3) The maintenance of the proper potential difference between the hollow cathode discharge plasma and the plasma of the main discharge chamber depends on the magnetic fields in the cathode discharge region. When these field lines do not lie across the baffle aperture, it is virtually impossible to achieve the desired impendance. In cases where the ambient fields from the main chamber do not provide sufficient impedance, supplemental fields from magnetic baffle assemblies are needed.

Quantitative evaluation of these three effects were not developed and will require much more detailed theoretical and experimental investigation.

The 15-cm-diam mercury multipole thruster performs better with two 2.7-cm-long side wall sections ($L/D = 0.34$) than it does with either one, three, or four. Extending the cathode chamber downstream into the main discharge region causes a local depletion of ion and electron densities. This flattens the ion beam profile and reduces the beam current.

This thruster exhibits propellant utilization efficiencies, discharge losses, and doubly-to-singly charged ion densities that are comparable to those observed in the SERT II and cusped magnetic field thrusters. Slight additional improvements in ion beam flatness and discharge losses of the multipole thruster are expected to accompany design changes that equalize the current density to each of the anodes.

Acknowledgment

This work was performed under NASA Grant NGR-06-002-112 to Colorado State University.

References

[1] Knauer, W., Poeschel, R.L., King, H.J., and Ward, J.W., "Discharge Chamber Studies for Mercury Bombardment Ion Thrusters," NASA CR-72440, Hughes Research Laboratories, Malibu, Calif., Sept. 1968.

[2] Masek, T.D., "Plasma Properties and Performance of Mercury Ion Thrusters," *AIAA Journal*, Vol. 9, Feb. 1971, pp. 205-212.

[3] Beattie, J.R., "Cusped Magnetic Field Mercury Ion Thruster," NASA CR-135047, Colorado State University, Fort Collins, Colo., July 1976.

[4] Kaufman, H.R., "Technology of Electron Bombardment Ion Thrusters," *Advances in Electronics and Electron Physics*, Vol. 36, 1974, Academic Press, Inc., N.Y., pp. 273-275.

[5] King, J.H., Poeschel, R.L., and Ward, J.W., "A 30 cm Low Specific Impulse, Hollow Cathode, Mercury Thruster," *Journal of Spacecraft and Rockets*, Vol. 7, April 1970, pp. 416-421.

[6] Isaacson, G.C. and Kaufman, H.R., "15 cm Multipole Gas Ion Thruster," *Journal of Spacecraft and Rockets*, Vol. 14, Aug. 1977, pp. 469-473.

[7] Beattie, J.R., "Numerical Procedure for Analyzing Langmuir Probe Data," *AIAA Journal*, Vol. 13, July 1975, pp. 950-952.

[8] Vahrenkamp, R.P., "Measurement of Doubly Charged Ions in the Beam of a 30 cm Mercury Bombardment Thruster," AIAA Paper 73-1057, Lake Tahoe, Nev., Oct. 31-Nov. 2, 1973.

[9] Wells, A.A., "Current Flow Across a Plasma 'Double Layer' in a Hollow Cathode Ion Thruster," AIAA Paper 72-418, April 1972.

[10] Robinson, R.S. and Kaufman, H.R., "Ion Thruster Technology Applied to a 30-cm Multipole Sputtering Ion Source," *AIAA Journal*, Vol. 15, May 1977, pp. 702-706.

[11] Longhurst, G.R., "The Diffusion and Collection of Electrons in Ion Thrusters," in *Mercury Ion Thruster Research – 1977*, edited by P.J. Wilbur, NASA CR-135317, Dec. 1977.